

## **Zirconium oxide based boron doped diamond electrochemical sensor and its application for determination of bronchodilator, anti-inflammatory and mucoregulator drug Acebrophylline**

Ramkishore Sharma<sup>a</sup>, Preeti Pandey\*<sup>b</sup>, Renu Nayar<sup>b</sup>

<sup>a</sup>School of Studies in Chemistry, Jiwaji University, Gwalior – 474011, India

<sup>b</sup>Dept of chemistry, D.P. Vipra College, Bilaspur- 49500, India

---

**Abstract:** A novel and very sensitive electrochemical sensor based on zirconium oxide (ZrO<sub>2</sub>) nanoparticles has been developed by modification of boron doped diamond electrode (BDDE). Electrochemical impedance spectra showed reduction of charge transfer resistance and higher electrocatalytic behaviour of the sensors. The electrochemical characteristic of the modified electrodes were characterized by scanning electron microscopy (SEM), X-ray diffraction (XRD) and electrochemical impedance spectroscopy (EIS). The electrochemical behaviour of Acebrophylline was studied at bare BDDE and ZrO<sub>2</sub>/BDDE using cyclic voltammetric (CV) and square-wave voltammetric (SWV) techniques. A well defined oxidation peak was observed in Britton-Robinson (BR) buffered solution. Variation of scan rate revealed that the electrode process is diffusion controlled. ZrO<sub>2</sub>/BDDE showed higher current response (CV, 63% and SWV, 67%) as compared to bare BDDE. ZrO<sub>2</sub>/BDDE showed a linear response for Acebrophylline over the concentration range of 25–250 µg/mL with the detection limit 11.98 µg/mL. This method was employed for quantification of Acebrophylline in six different pharmaceutical formulations.

**Keywords:** ZrO<sub>2</sub>/BDDE Sensor; Electrochemical impedance spectroscopy; XRD; SEM; Acebrophylline; Voltammetry; Pharmaceutical formulations.

---

\*Corresponding author e-mail: preeti.pc2010@gmail.com

Tele. No.: 91-9425712252, 9977413760

---

### **I. Introduction**

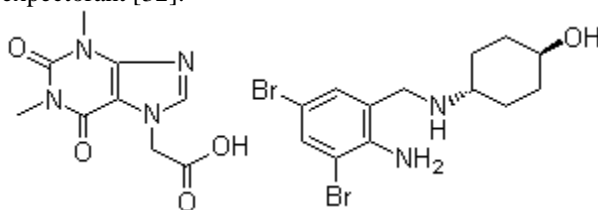
In the last decades electrochemical sensors have been increasingly developed for many applications in environmental monitoring, pharmaceutical analysis and clinical chemistry due to their specificity, sensitivity, accuracy and portability [1–3]. The performance of electrochemical sensors mainly depends on the physical and chemical characteristics of the materials, including shape and structure, employed for the construction of the sensors. Conventional carbon-based materials including, carbon paste, porous carbon, glassy carbon and carbon nanotubes have been widely employed as electrochemical sensor due to simple preparation methods, large positive potential ranges and suitability for chemical modification [4–7]. However, traditional carbon-based electrodes still suffer some drawbacks, such as electrode fouling, which limits their long-term stability and leads to frequent polishing or disposal of the electrode.

In recent years, conductive diamond electrodes for electrochemical applications have been a major focus of research and development. The impetus behind such endeavors could be attributed to their wide potential window, low background current, chemical inertness and mechanical durability. In the tetrahedral diamond lattice, each carbon atom is covalently bonded to its neighbours forming an extremely robust crystalline structure. Some carbon atoms in the lattice are substituted with boron to provide electrical conductivity. Modification strategies of doped diamond electrodes with metallic nanoparticles and/or electro polymerized films are of importance to impart novel characteristics or to improve the performance of diamond electrodes.

Boron-doped diamond (BDD) electrode is one new kind of electrode, are gaining big researching interests. BDD electrodes possess many outstanding properties, including wide electrochemical potential window, resistance to thermal shock, extreme electrochemical stability and corrosion stability in aggressive media. This makes them also totally different to common electrode materials such as gold, platinum or mixed metal oxide DSA-type electrodes. The wider potential window and lower background currents make the BDD material very attractive for electrochemical analysis experiments, particularly suitable for deep anodic oxidation [8]. Reactions occurring in higher potential ranges can now be analyzed which could not be analyzed on traditional electrode surfaces such as Au and Pt. The lower background current allows for higher sensitivity and

lower detection limits. BDD is mechanical robust and biocompatible which makes the material a suitable electrode material for various applications. Therefore, BDD electrodes have been widely employed for the construction of various electrochemical sensors and biosensors [9–12]. On the other hand zirconium oxide is an environmentally friendly and naturally available element.  $ZrO_2$  adopts a monoclinic crystal structure at room temperature and transitions to tetragonal and cubic at higher temperatures. Over the last few years, zirconium oxide has been utilised in different kinds of sensors due to energy band gap, high electrical conductivity, chemical stability and mechanical strength and has found a wide range of interesting environmental and clinical applications [13–30]. Zirconium oxide is relatively un-reactive chemically but when heated with carbon, it converts to zirconium carbide. Because of their unique electrochemical properties, it has been used for electrochemical detection of DNA hybridization by zirconia modified diamond electrode [31]. Therefore,  $ZrO_2$ /BDDE can be used for a plethora of applications.

Acebrophylline, is 1, 2, 3, 6-tetrahydro-1, 3-dimethyl-2, 6-dioxo-7H-purine-7-acetic acid -with trans-4-[(2-amino-3,5-dibromophenyl)methyl]amino]cyclohexanol. Acebrophylline (Scheme -1) is a drug showing specific bronchodilator, anti-inflammatory, and mucoregulator activity. It is the salt obtained by reaction of equimolar amounts of Theophylline-7-acetic acid, a xanthine derivative with specific bronchodilator activity and Ambroxol, a mucolytic and expectorant [32].



**Scheme 1**

Literature survey revealed that various analytical methods have been reported for assay of Acebrophylline like spectrophotometric [33–35], HPLC [36–39] and HPTLC [40, 41], have been reported for the determination of Ambroxol HCl and Theophylline -7- acetic acid, individually and in combination with some other drugs. However, spectroscopic and chromatographic are commonly utilised but these methods involve several time consuming extraction, purification and derivatization steps and uses of excess amounts of solvents, reagents and sophisticated instrumentation restrict their use in routine analysis. On the other hand electrochemical techniques are less time consuming, highly sensitive and inexpensive hence, can be considered as a strong alternative to the above mentioned methods [42–51].

Present study reports an electrochemical method for the determination of Acebrophylline at boron doped diamond electrode (BDDE) and  $ZrO_2$  modified BDDE electrodes using square-wave and cyclic voltammetry. BDDE modified with zirconium oxide ( $ZrO_2$ ) nanoparticles to improve the sensitivity of electrodes for electrochemical detection. Charge transfer resistance was investigated using electrochemical impedance spectroscopy (EIS). The electrochemical characteristic of the modified electrodes were characterized by scanning electron microscopy (SEM) and X-ray diffraction (XRD) techniques.

## II. Experimental Section

### 2.1 Apparatus

Electrochemical measurements were carried out using at Autolab potentiostat-galvanostat 302N (Netherlands) with software NOVA 1.8. The utilized electrodes were BDDE and  $ZrO_2$ /BDDE as working electrodes, graphite rod an auxiliary electrode and Ag/AgCl (3M KCl) as reference electrode. All pH measurements were made on a Decible DB-1011 digital pH meter fitted with a glass electrode and a saturated calomel electrode as reference which was pre-standardized with buffers of known pH. Electron Impedance Spectroscopic (EIS) study was carried out at Autolab potentiostat-galvanostat 302N (Netherlands) with software NOVA 1.8 using FRA modules.

### 2.2 Reagents and chemicals

ZrO<sub>2</sub> nanopowder (90–250 nm, 99.8% purity) was procured from Sigma Aldrich (USA). Acebrophylline standard (98.95%, purity) was provided by Ajanta Pharmaceuticals Pvt. Ltd. (India). Acebrophylline-containing tablets (labelled 100 mg, Acebrophylline/Capsule) from different companies were procured from commercial sources. Ultra pure water, obtained from Milli-Q purification system (Millipore Corp., Milford, MA, USA). All other chemicals used were of analytical grade and used without further purification.

### 2.3 Analytical procedure

Standard solution of Acebrophylline (1 mg/mL) was prepared by dissolving standard in methanol and further dilutions were prepared with BR buffer to get final concentration in the working range (25–250 µg/mL). A series of Britton-Robinson (BR) buffer (2.0–12.0 pH) was prepared in ultra-pure water and used as supporting electrolytes. For electrochemical measurements, a known volume of the analyte sample was added in voltammetric cell and total volume made up to 10 mL with supporting electrolyte; this solution was deoxygenated with pure nitrogen gas for 50 s. The voltammograms were recorded by applying positive potential scan from 0.1–1.6 V, frequency 50 Hz, pulse amplitude 50 mV/s and scan increment 10 mV/s. All measurements were carried out at room temperature.

### 2.4 Fabrication of ZrO<sub>2</sub>/BDDE electrode

Prior to use BDDE was polished with 0.3 µm alumina slurry and washed with deionised water. The cleaned BDEE was gently blown under a nitrogen stream. ZrO<sub>2</sub> nanoparticles were dispersed in dimethylformamide (DMF) at a concentration of 2 mg/mL. ZrO<sub>2</sub>/BDEE modified electrode was fabricated by casting 10 µL of ZrO<sub>2</sub> suspension on the BDEE surface and dried at room temperature. ZrO<sub>2</sub> modified BDEE surface was cleaned after the measurements by physical removal of the cast film followed by polishing with 0.3 µm alumina slurry and ultrasonic cleaning for 2 min.

### 2.5 Characterization of the electrode

#### 2.5.1 Electrochemical impedance spectroscopy

The capacity of electron transfer of BDDE and the modified electrode (ZrO<sub>2</sub>/BDDE) was investigated using electrochemical impedance spectroscopy. Fig. 1A represents the Nyquist diagram of Acebrophylline (100 µg/mL) in BR buffer solution (3.8 pH) at an AC amplitude of 10 mV and frequency of 1–1000 Hz at BDDE and at ZrO<sub>2</sub>/BDDE. All the Nyquist plots represent a relatively depressed semi circle at high frequencies and a line with a slope at low frequency. This implies that the redox process occurred in the mixed regime of charge and mass transfer. By fitting the data using an appropriate equivalent circuit (Fig.1 B), the values of charge transfer resistance were determined and found to be 18.8 k Ω at BDDE and 10.6 k Ω at ZrO<sub>2</sub>/BDDE. The lower charge transfer resistance of ZrO<sub>2</sub>/BDDE indicated that ZrO<sub>2</sub> has higher electrocatalytic behaviour towards the electro-oxidation of Acebrophylline. The decrease in the charge transfer resistance can be related to the electrode coverage and is given by the following equation:

$$(1-\Theta) = R_{CT}^0/R_{CT} \quad (1)$$

Where  $\Theta$  is the apparent electrode coverage and  $R_{CT}^0$  and  $R_{CT}$  is the charge transfer resistance measured at bare and modified glassy carbon electrode [52]. In the equivalent circuit  $R_s$ ,  $C_{dl}$ ,  $R_{ct}$ ,  $W$  and  $Q$  represents the solution resistance, double layer capacitance, charge transfer resistance, the Warburg impedance and the constant phase element. A constant phase element was used instead of the pure capacitance because of the depression in the high frequency semicircle and again the line that appeared at low frequency is because of diffusion of the electroactive species in the bulk of the solution.

#### Figure 1

#### 2.5.2 X-ray diffraction

The X-ray diffraction pattern of zirconia nanoparticles is shown in Fig. 2, the diffraction peaks are absorbed at  $2\theta$  ranges between 10°-70°. The prominent peaks have been utilized to estimate the grain size of sample with the help of Scherer equation [53]  $D = K\lambda/(\beta \cos \theta)$  where  $K$  is constant (0.9),  $\lambda$  is the wavelength ( $\lambda = 1.5418 \text{ \AA}$ ) (Cu  $K\alpha$ ),  $\beta$  is the full width at the half maximum of the line and  $\theta$  is the diffraction angle. About 30 mg of each powdered sample was kept in a glass sample holder and pressed using a glass slide to obtain a uniform distribution. The  $2\theta$  Bragg angles were scanned over a range of 20-85° at a rate of 2° per minute with a 0.02° angular resolution. The pure ZrO<sub>2</sub> powders exhibit two broad peaks at  $2\theta$  angles around 28.29° and 31.57°.

which correspond to the diffraction of the (100) and (64) respectively. It's indicated that the ZrO<sub>2</sub> has crystalline in nature.

## Figure 2

### 2.5.3 Scanning electron microscopy

Further characterization measurements were conducted for defining the morphology of the zirconium oxide nanoparticles. It should be mentioned that a minimal exposure of the obtained product to air, caused the powder to burn. The surface morphological study of the ZrO<sub>2</sub>/GCE sensor was carried out by scanning electron microscopy (SEM) using Zeiss EV0 50 instrument. In any case the oxygen level, as measured by elemental analysis, was low even in cases in which we had to expose the sample for a short period to air. Figure 3 depicts the SEM image of the ZrO<sub>2</sub> precursor. The morphology of the zirconium dioxide consisted mostly of spheres. The average size of the zirconium oxide nanoparticles was measured by using the scion image program averaged over 200 particles. The average size of the ZrO<sub>2</sub> particles was found to be 100 ± 5 nm. However, it seems that even these particles are aggregates of smaller, 20–40 nm, particles. In the modification of bare GCE by using zirconium oxide nanoparticles not only increases the electroactive surface area of the electrode but also improves the electron transfer rate between the electrode surface and the bulk solution.

## Figure 3

## III. Results And Discussion

### 3.1 Enhancement study of Acebrophylline at ZrO<sub>2</sub>/BDDE and comparison with BDDE

The electrochemical behaviour of Acebrophylline at ZrO<sub>2</sub>/BDDE and BDDE was investigated using cyclic and square-wave voltammetry. Acebrophylline exhibited a well defined oxidation peak at the both electrodes. The electroanalytical performance of ZrO<sub>2</sub>/BDDE was advantageous over that observed at the bare BDDE. The cyclic voltammograms of Acebrophylline showed 63% enhancement in the oxidation peak current at ZrO<sub>2</sub>/BDDE (Fig. 4, curve c) as compared to a bare BDDE (Fig. 4, curve b). Whereas; square-wave voltammograms showed 67% enhancement in the oxidation peak current at ZrO<sub>2</sub>/BDDE (Fig. 5, curve c) as compared to a bare BDDE (Fig. 5, curve b). At modified electrode peak potential was also shifted towards negative side, indicated that the electron transfer kinetics was much higher with ZrO<sub>2</sub>/BDDE. This is the fact that further improving the sensitivity for voltammetric measurement.

## Figure 4

## Figure 5

### 3.2 Effect of supporting electrolyte and pH

Preliminary investigations were carried out to obtain the most suitable supporting electrolyte and pH value for obtaining the best response of Acebrophylline. Therefore various supporting electrolyte like KCl, phosphate buffer, acetate buffer, citrate buffer, borate buffer and BR buffer were tested. However the best results were obtained in BR buffer with respect to the signal enhancement and the symmetric peak profile. The effect of varying pH (2.5–12) of BR buffer on the peak current of Acebrophylline was investigated at constant concentration. Optimum peak current was achieved at pH 3.8, with the rise in pH the peak current decreases due to pH dependence of half wave potential which indicates the involvement of protons in the electrode process and finally dislocated in alkaline pH due to lower number of available protons (Fig. 6A). Thus, BR buffer (3.8 pH) was selected for the study purpose. With the rise in pH, the peak potential was also shifted towards negative side (Fig. 6B). This reveals that the pH of the supporting electrolyte exerted a significant influence on the electrooxidation of Acebrophylline. The dependence of peak current and peak potential on pH can be expressed by the following expressions:

$$i_p / \mu\text{A} = -0.0834 \text{ pH} + 0.7318; r^2 = 0.8912 \quad (2)$$

$$E_p / \text{V (vs. Ag/AgCl)} = -0.0481 \text{ pH} - 1.0941; r^2 = 0.9914 \quad (3)$$

An experimental slope of 0.0481 V/pH was obtained which is close to the expected slope 0.0590 V/pH (Classical Nernstain two-electron, two-proton process), which proposes that the no. of electrons and protons participating in the oxidation of Acebrophylline are same. The difference between theoretical and experimental slope can be related to the quasi-irreversible mechanism.

## Figure 6

### 3.3 Effect of scan rate

To study the effect of scan rate on the oxidation peak current of Acebrophylline at ZrO<sub>2</sub>/BDDE, voltammograms of Acebrophylline (100 µg/mL) were recorded at different scan rate over the range 10–200 mV/s (Fig. 7A). Acebrophylline at ZrO<sub>2</sub>/BDDE exhibits a single well defined oxidation peak at 1.1 V (vs. Ag/AgCl). Since no peak was observed in reverse scan corresponding to the anodic peak, which exhibits the irreversible nature of the electrode process. The peak potential shifts towards right-handed with the increase in the scan rate, again confirming the irreversible nature of the oxidation process, which can be expressed by the equation:

$$E_p = E^0 + RT(1-\alpha)nF \{ \ln(k_s/D^{1/2}) - 0.5 \ln[(1-\alpha)nFv/RT] - 0.78 \} \quad (4)$$

Where, E<sup>0</sup> is the standard electrode potential, D is the diffusion coefficient, v is the scan rate, F is the faraday constant, R is the as constant and T is the room temperature. A linear plot of current (i<sub>p</sub>) vs. square root of scan rate (v<sup>1/2</sup>) is obtained when the process is diffusion controlled, whereas the adsorption controlled process results in a linear plot of i<sub>p</sub> vs. v [54]. In the present experiment a linear relationship between i<sub>p</sub> and v<sup>1/2</sup> is obtained suggesting the diffusion of Acebrophylline at the surface of ZrO<sub>2</sub>/BDDE (Fig. 7B), which can be expressed by the following equation:

$$i_p / \mu A = 0.5035 v^{1/2} (\text{mV/s}) - 1.3768; r^2 = 0.9935 \quad (5)$$

Again a linear relationship was observed between log i<sub>p</sub> and log v (Fig. 7C), corresponding to the equation:

$$\log i_p = 0.5067 \log v - 0.3730; r^2 = 0.9988 \quad (6)$$

The slope of 0.5067 is close to the expected value of 0.5 for a purely diffusion controlled irreversible anodic reaction [55].

### Figure 7

### 3.4 Calibration graph and detection limit

In order to see the feasibility of the explored method for the quantification of Acebrophylline, the relationship between the oxidative peak current and concentration was evaluated using square-wave voltammetry at ZrO<sub>2</sub>/BDDE. Square-wave voltammograms obtained with increasing amounts of Acebrophylline showed that peak current increased linearly with increasing concentration (Fig. 8A). Since the modified electrode greatly improves the sensitivity for the determination of the Acebrophylline, it signifies the electrocatalytic activity of the ZrO<sub>2</sub>/BDDE for the oxidation of Acebrophylline. Linear calibration curve is obtained for Acebrophylline over the range of 25–250 µg/mL (Fig. 8B), which can be expressed by the following equation:

$$i_p / \mu A = 0.0040 (\mu\text{g/mL}) + 0.2649; r^2 = 0.9953 \quad (7)$$

Limit of detection (LOD, 11.98 µg/mL) and limit of quantification (LOQ, 36.29 µg/mL) estimated as 3S/m and 10S/m respectively. Where “S” is the standard deviation and “m” is the slope of the calibration curve. The square-wave voltammetric method validation parameters for the standard linearity have been calculated and summarised in Table 1.

### Figure 8

### Table 1

### 3.5 Stability and reproducibility of the modified electrode

Stability of the ZrO<sub>2</sub> modified electrode for the determination of Acebrophylline was examined by measuring the current response at fixed concentration of Acebrophylline (100 µg/mL) by proposed square-wave

voltammetric method. The modified electrode was used daily and stored in air at room temperature. The modified electrode showed a deviation in peak current of Acebrophylline by 3.98 % after a single day, while after a week modified electrode showed a relative standard deviation of 6.73 %. These result indicated that modified electrode possess good stability.

The reproducibility of the ZrO<sub>2</sub> modified electrode was evaluated by repetitive measurements (n=6) of Acebrophylline (100 µg/mL). The corresponding relative standard deviation of 2.43 % confirms that results are satisfactorily reproducible. In order to examine intraday (repeatability) and interday (reproducibility) response, square-wave voltammograms were recorded at ZrO<sub>2</sub>/BDDE. The experimental results showed that the intraday current response deviated by 3.79 % and interday current response by 4.89 %. These results indicated that ZrO<sub>2</sub>/BDDE possess adequate reproducibility for determination of Acebrophylline.

### **3.6 Determination of Acebrophylline in different pharmaceutical formulations**

The ZrO<sub>2</sub> modified electrode was successfully applied for the determination of Acebrophylline in different pharmaceutical formulations without the necessity for samples pretreatment or time-consuming extraction steps prior to analysis. Acebrophylline contents were determined in six different formulations i.e. AB-FLO (Mfd. by Lupin), Ascovent (Mfd. by Glenmark), Erophylin (Mfd. by Micro Labs), Macphyllin (Mfd. by Macleod's), Mucophyline (Mfd. by Cipla) and Ventibro (Mfd. by FDC Ltd.). An accurately weighed amount of powder was transferred to 10 mL volumetric flask containing 5 mL of methanol, to ensure complete solubility of the drug contents of the flask were sonicated for 5 min and its volume was made up to mark with methanol and centrifuged at 3200 rpm for 5 min. Clear supernatant liquid was withdrawn and diluted with BR buffer of pH 3.8, so that final concentration came under working range. The square-wave voltammograms were recorded under previously optimized conditions. The concentration of Acebrophylline obtained by proposed method in different pharmaceutical formulations was compared with labelled claimed and is summarized in Table 2. Results show that Acebrophylline contents for all pharmaceutical formulation fall within claimed amount with error less than ± 6%, indicating that the proposed voltammetric method can be applied for determination of Acebrophylline in pharmaceutical formulations.

**Table 2**

## **IV. Conclusion**

A novel and simple strategy for the selective determination of Acebrophylline at ZrO<sub>2</sub>/BDDE is presented in this paper. In this work it was found that modification of the BDDE with ZrO<sub>2</sub> significantly enhanced the activity of the electrode surface. The electrocatalytic behaviour of ZrO<sub>2</sub>/BDDE was studied by EIS, which showed reduction of charge transfer resistance and higher electrocatalytic behaviour of the sensor. Enhancement study was performed using SWV and CV techniques. ZrO<sub>2</sub>/BDDE showed (CV 63% and SWV 67%) current enhancements when compared with the bare BDDE. Calibration plot reveals linearity within the range of 25–250 µg/mL with correlation coefficient of 0.9953. Lower limit of detection (11.98 µg/mL) proved the sensitivity of the proposed method. Voltammetric study of Acebrophylline at different scan rates revealed the irreversible and diffusion controlled reaction process. The proposed sensor can be successfully applied to the detection of Acebrophylline in different pharmaceutical formulation.

## **Acknowledgements**

Authors acknowledge their work to Dayalbagh Educational Institute, Dayalbagh, Agra, (India) to provide lab facility.

## **References**

- [1]. R. Jain, R. Sharma, J. Appl. Electrochem., **42**, 341 (2012).
- [2]. R. Shrivastava, R. Sharma, S.P. Satsangee, R. Jain, J. Electrochem. Soc., **159**, 795 (2012).

- [3]. R.N. Goyal, V.K. Gupta, and S. Chatterjee, *Biosens. & Bioelect.*, **24**, 3562 (2009).
- [4]. R.N. Goyal, V.K. Gupta, S. Chatterjee, *Talanta*, **76**, 662 (2008).
- [5]. R.N. Goyal, M. Oyama, V.K. Gupta, S.P. Singh, R.A. Sharma, *Sens. Actu. B: Chem.*, **134**, 816 (2008).
- [6]. M. Pan, G. Fang, Z. Duan, L. Kong, S. Wang, *Biosen. Bioelec.*, **31**, 11 (2012).
- [7]. A. Gholizadeha, S. Shahrokhiana, A.I. Zada, S. Mohajerzadehd, M. Vosoughia, S. Darbarid, Z. Sanaeed, *Biosen. Bioelec.*, **31**, 110 (2012).
- [8]. Yu.V. Pleskov, *Elektrokimiya Almaza (Electrochemistry of Diamond)*, URSS, Moscow, Russia, 2003.
- [9]. V. Suryanarayanan, Y. Zhang, S. Yoshihara, T. Shirakashi, *Electroanalysis*, **17**, 925 (2005).
- [10]. E. O. Faria, A.C.V. Lopes Junior, D.E. Pires Souto, F.R. Figueiredo Leite, F.S. Damos, R. C. Silva Luz, A.S. Santos, D.L.Franco, W.T.P. Santos, *Electroanalysis*, **24**, 1141 (2012).
- [11]. B.C. Lourencao, R.A. Medeiros, R.C. Rocha-Filho, L.H. Mazo, O. Fatibello-Filho, *Talanta*, **78**, 748 (2009).
- [12]. E.F. Batista, E.R. Sartori, R.A. Medeiros, R.C. Rocha-Filho, O. Fatibello-Filho, *Analytical Letters*, **43**, 1046 (2010).
- [13]. N. Miura, H. Kurosawa, M. Hasei, G.Y. Lu, N. Yamazoe, *Solid State Ionics*, **86**, 1069 (1996).
- [14]. G.Y. Lu, N. Miura, N. Yamazoe, *Sens. Actuators B: Chem.*, **35**, 130 (1996).
- [15]. N. Miura, G.Y. Lu, N. Yamazoe, H. Kurosawa, M. Hasei, *J. Electrochem. Soc.*, **143**, L33 (1996).
- [16]. G.Y. Lu, N. Miura, N. Yamazoe, *J. Mater. Chem.*, **7**, 1445 (1997).
- [17]. S. Zhuiykov, T. Ono, N. Yamazoe, N. Miura, *Solid State Ionics*, **152**, 801 (2002).
- [18]. N. Miura, S. Zhuiykov, T. Ono, M. Hasei, N. Yamazoe, *Sens. Actuators B: Chem.*, **81**, 222 (2002).
- [19]. S.Q. Liu, J.J. Xu, H.Y. Chen, *Bioelectrochemistry*, **57**, 149 (2002).
- [20]. N. Miura, M. Nakatou, S. Zhuiykov, *Sens. Actuators B: Chem.*, **93**, 221 (2003).
- [21]. S. Liu, Z. Dai, H. Chen, H. Ju, *Biosen. Bioelect.*, **19**, 963 (2004).
- [22]. P. Elumalai, N. Miura, *Solid State Ionics*, **31**, 2517 (2005).
- [23]. N. Miura, J. Wang, M. Nakatou, P. Elumalai, S. Zhuiykov, M. Hasei, *Sens. Actuators B: Chem.*, **114**, 903 (2006).
- [24]. M. Nakatou, N. Miura, *Sens. Actuators B: Chem.*, **120**, 57 (2006).
- [25]. T. Zhongqiang, Y. Ruo, C. Yaqin, X. Yi, C. Shihong, J. Biotechnology, **128**, 567 (2007).
- [26]. P. Elumalai, V. Plashnitsa, T. Ueda, N. Miura, *Electrochem. Commun.*, **10**, 745 (2008).
- [27]. V. Plashnitsa, T. Ueda, P. Elumalai, N. Miura, *Sens. Actuators B: Chem.*, **130**, 231 (2008).
- [28]. V. Plashnitsa, P. Elumalai, Y. Fujio, N. Miura, *Electrochim. Acta*, **54**, 6099 (2009).
- [29]. M. Das, G. Sumana, R. Nagarajan, B. D. Malhotra, *Appl. Phys. Lett.*, **96**, 133 (2010).
- [30]. X. Liang, S. Yang, J. Li, H. Zhang, Q. Diao, W. Zhao, G. Lu, *Sens. Actuators B:*, **158**, 1(2011).
- [31]. B. Liu, J. Hu, J.S. Foord, *Electrochem. Commun.*, **19**, 46 (2012).
- [32]. S.R. Dhaneshwar, V.N. Jagtap, *J. Basic. Appl. Sci. Res.*, **1**, 1884 (2011).
- [33]. N.M. Gowekar, V.V. Pande, A.V. Kasture, A.R. Tekade, J.G. Chandorkar, *Pak. J. Pharm. Sci.*, **20**, 250 (2007).
- [34]. P.S. Lakshmana, A.A. Shirwaikar, S. Annie, D. Kumar, Aravind, *Ind. J. Pharm. Sci.*, **70**, 236 (2008).
- [35]. A.O. James, N. Kanji, *Clin. Chem.*, **24**, 367 (1978).
- [36]. A. Trivedi, L. Banerjee, *J.vPharm. Research*, **3**, 1398 (2010).
- [37]. Bhatia, Neela, *J. Pharm. Sci.*, **70**, 603 (2008).
- [38]. K. Veni, S.N. Meyyanathan, *Research J. Pharm. Tech.*, **1**, 366 (2008).
- [39]. K.A. Shaikh, S.D. Patil, *J. Pharm. Biomed. Anal.*, **48**, 1481 (2008).
- [40]. P.S. Jain, *J. Chromatogr. Sci.*, **8**, 45 (2010).
- [41]. N.M. Gowekar, V.V. Pande, A.V. Kasture, A.R. Tekade, J.G. Chandorkar, *Asian J. Chem.*, **19**, 1487, (2007).
- [42]. R.N. Goyal, V.K. Gupta, S. Chatterjee, *Biosens. Bioelectron.*, **24**, 1649 (2009).
- [43]. R. Jain, V. K. Gupta, N. Jadon, and K. Radhapyari, *Anal. Biochem.*, **407**, 79 (2010).
- [44]. R. Jain, V. K. Gupta, N. Jadon, and K. Radhapyari, *J. Electroanal. Chem.*, **648**, 20 (2010).
- [45]. V.K. Gupta, R. Jain, K. Radhapyari, N. Jadon, S. Agarwal, *Anal. Biochem.*, **408**, 179(2011). [46] V.K. Gupta, R. Jain, S. Agarwal, R. Mishra, A. Dwivedi, *Anal. Biochem.*, **410**, 266 (2011).
- [46]. R. Jain, R. Sharma, *J. Electrochem. Soc.*, **160**, H1 (2013).
- [47]. R. Jain, R. Sharma, R. K. Yadav, R. Shrivastava, *J. Electrochem. Soc.*, **160**, H179 (2013).
- [48]. R.N. Goyal, V.K. Gupta, M. Oyama, N. Bachheti, *Talanta*, **72**, 976 (2007).
- [49]. R. Jain, and R. Sharma, *J. Phar. Anal.*, **2**, 98 (2012).

- [50]. R. Jain, and R. Sharma, *J. Phar. Anal.*, **2**, 98 (2012).  
 [51]. E. Sabatani, I. Rubinstein, *J. Phys. Chem.*, **91**, 6663 (1987).  
 [52]. S. Mikoshiba, S. Murai, H. Sumino, S. Hayase, *Chem. Lett.*, **11**, 1156 (2002).  
 [53]. T. Laixing, F. wang, Y. Y. Mao, L. P. Wang, and B. X. Ye, *J. Chin. Chem. Soci.*, **56**, 303 (2009).  
 [54]. S. Yang, R. Yang, G. Li, J. Li, and L. Qu, *J. Chem Sci.*, **122**, 919 (2010).

**Table 1:** Square-wave voltammetric method validation parameters for standard linearity.

Linearity parameters	Results
Slope	0.0040
Standard deviation	0.0001
Intercept	0.2649
Standard deviation	0.0145
Correlation coefficient	0.9953
Standard error of estimation	0.0191
Sum of squares of regression	0.4654
Sum of squares of residuals	0.0022
Limit of detection ( $\mu\text{g/mL}$ )	11.98
Limit of quantification ( $\mu\text{g/mL}$ )	36.29

**Table 2:** Determination of Acebrophylline in different pharmaceutical formulations by proposed square-wave voltammetric methods.

Capsules	Amount labelled (mg)	Amount found* (mg)	Std. Dev.	(%) CV	(%) Error
AB-FLO	100	94.7	4.412	4.66	- 5.3
Ascovent	100	95.3	7.421	7.78	- 4.7
Erophylin	100	100.8	3.251	3.22	+ 0.8
Macphyllin	100	99.8	5.345	5.35	- 0.2
Mucophylline	100	96.2	8.010	8.33	- 3.8
Ventibro100	102.2	3.869	3.79	+2.2	

\*Amount found represents the average of six observations (n = 6).

### Figure captions

**Figure 1:** Nyquist plots of Acebrophylline (100  $\mu\text{g/mL}$ ) at BDDE (A, curve a) and  $\text{ZrO}_2/\text{BDDE}$  (A, curve b) and corresponding equivalent circuits used for the determination of charge transfer resistance (B).

**Figure 2:** X-ray diffraction patterns of the pure zirconium oxide nanoparticles.

**Figure 3:** Scanning electron microscopy of zirconium oxide nanoparticles.

**Figure 4:** Cyclic voltammograms of Acebrophylline at  $\text{ZrO}_2/\text{BDDE}$  (curve c), at BDDE (curve b) and blank (curve a).

**Figure 5:** Square-wave voltammograms of Acebrophylline at  $\text{ZrO}_2/\text{BDDE}$  (curve c), at BDDE (curve b) and blank (curve a).

**Figure 6:** Effect of different pH on peak current of Acebrophylline (A) and peak potential shift (B).

**Figure 7:** Cyclic voltammograms of Acebrophylline (100  $\mu\text{g/mL}$ ) at scan rates 10–200  $\text{mV/s}$  (A curves a–h), plot of  $v^{1/2}$  vs.  $i_p$  (B) and plot of  $\log v$  vs.  $\log i_p$  (C).

**Figure 8:** Square-wave voltammograms of Acebrophylline at different concentration levels, 25–250  $\mu\text{g/mL}$  (A curves a–i), at  $\text{ZrO}_2/\text{BDDE}$  and plot of concentration vs. current (B).



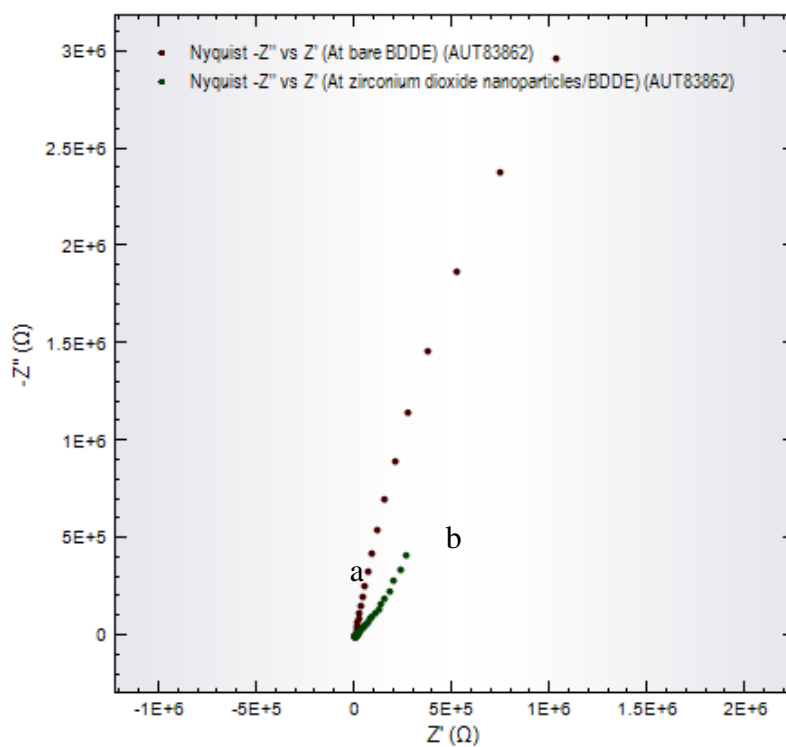


**Figure 1A**

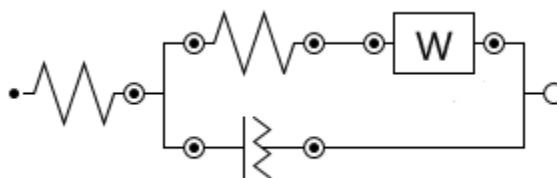


**Figure 1B**

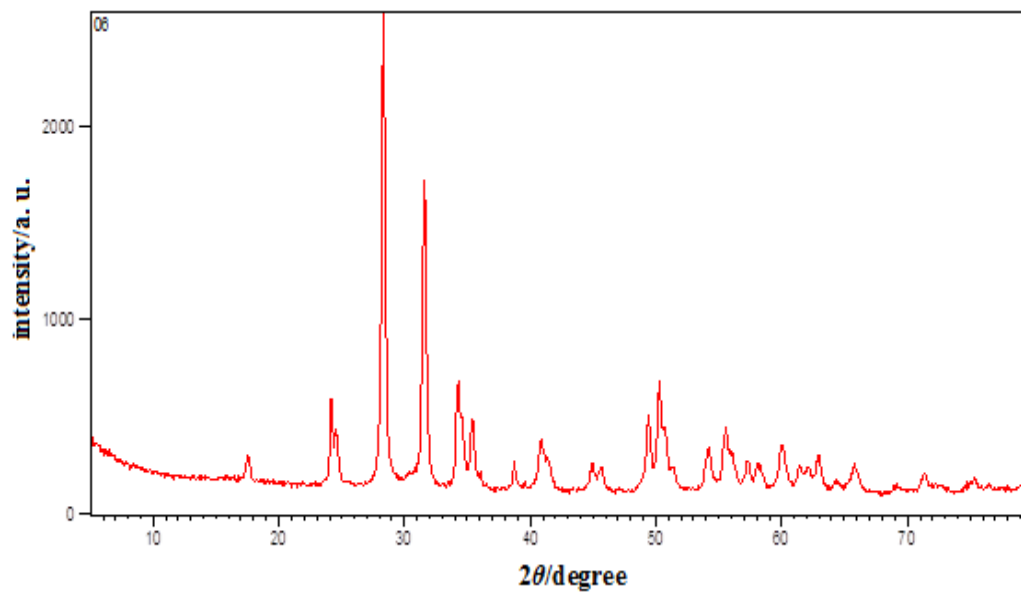


**Figure 2**

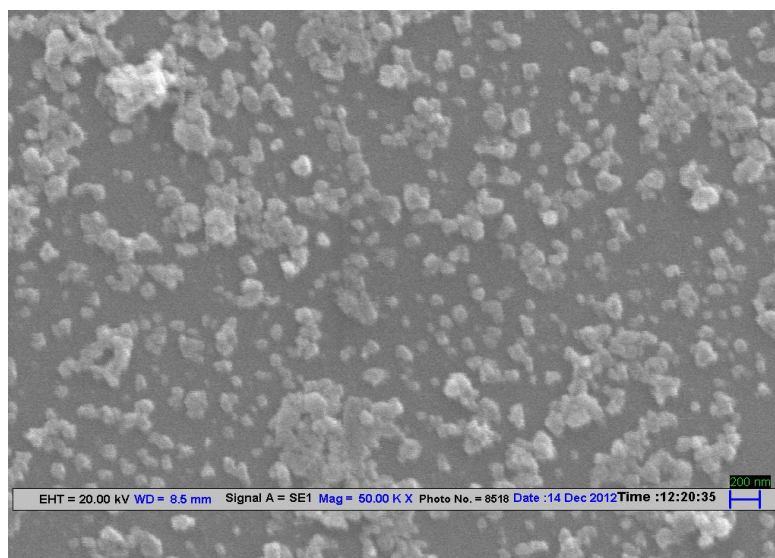


**Figure 3**

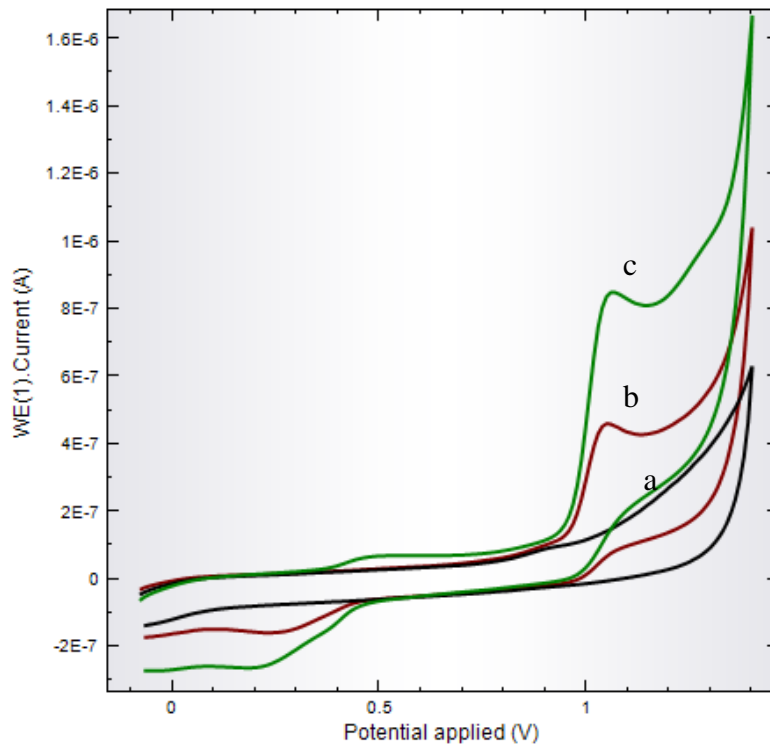


**Figure 4**

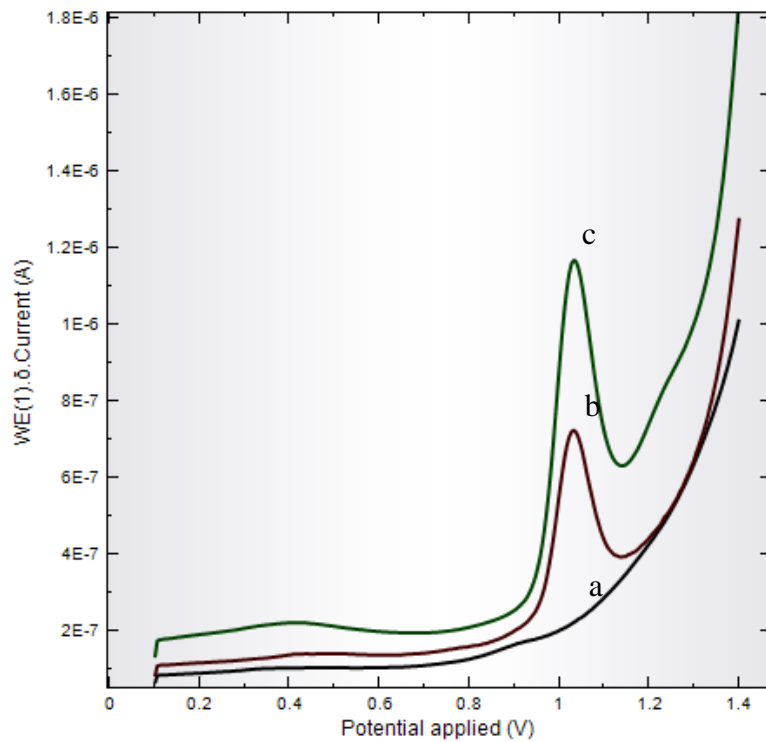


**Figure 5**

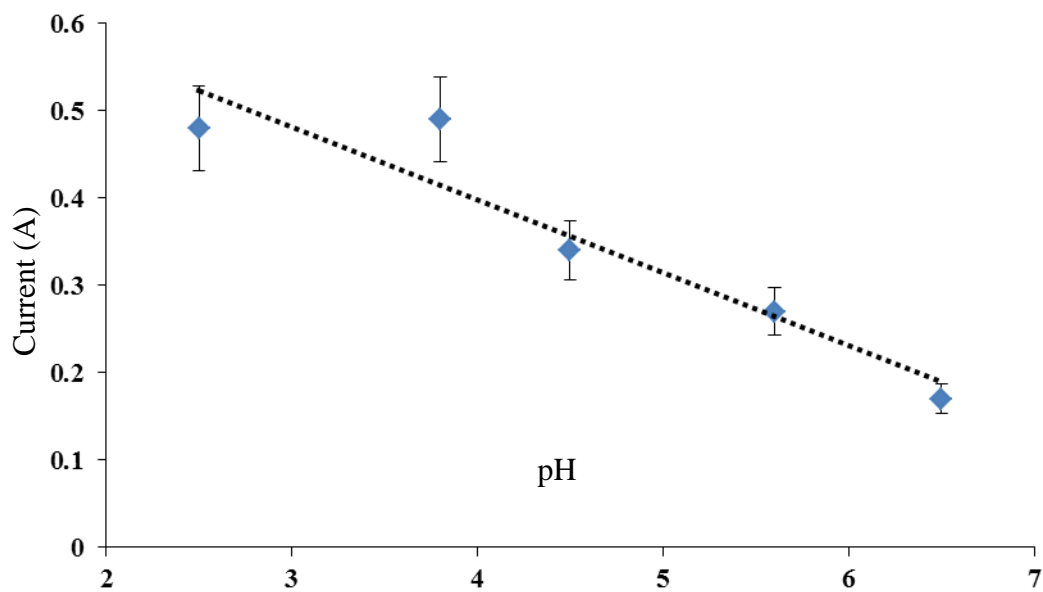


**Figure 6A**

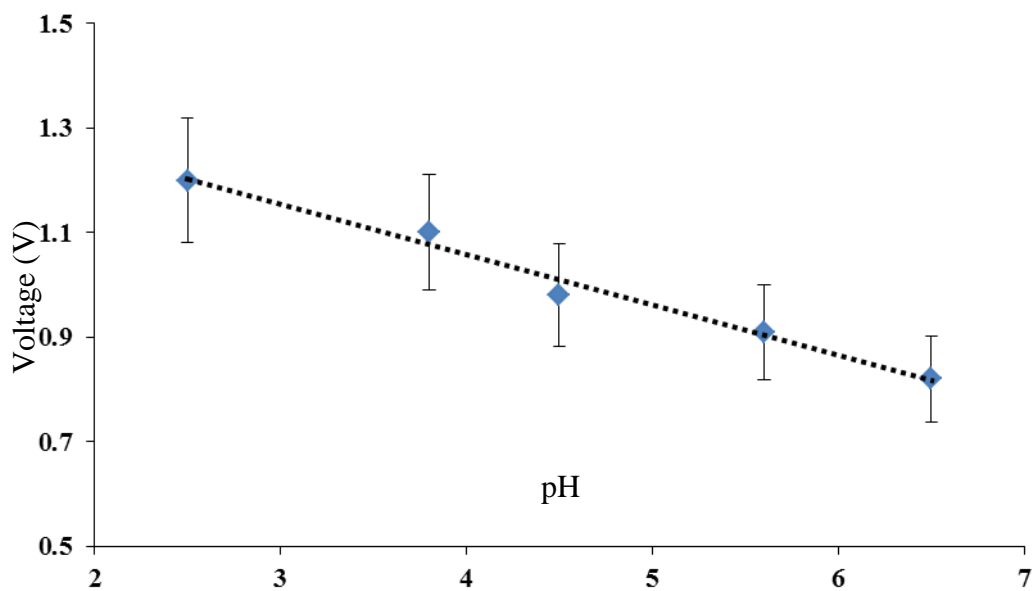


**Figure 6B**

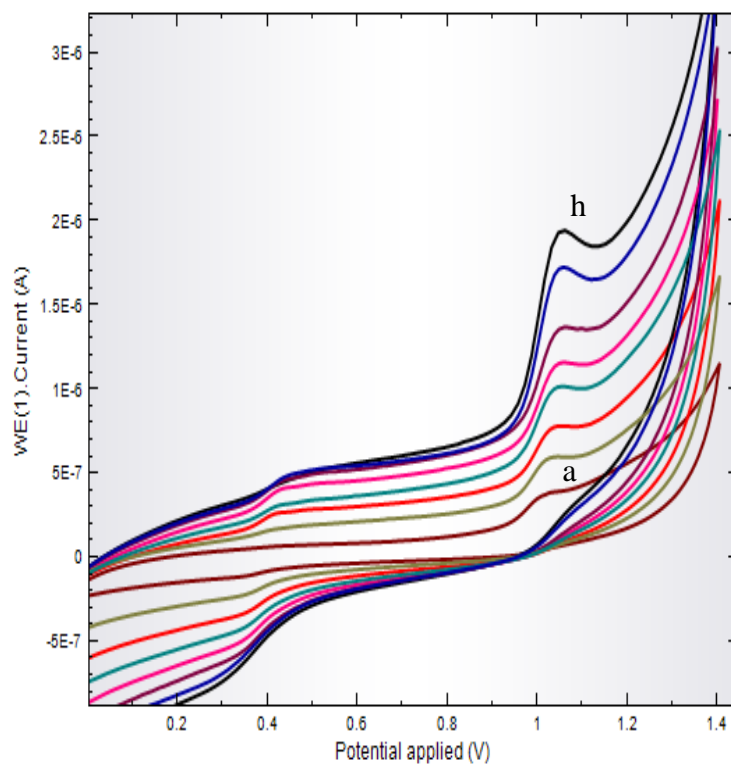


**Figure 7A**

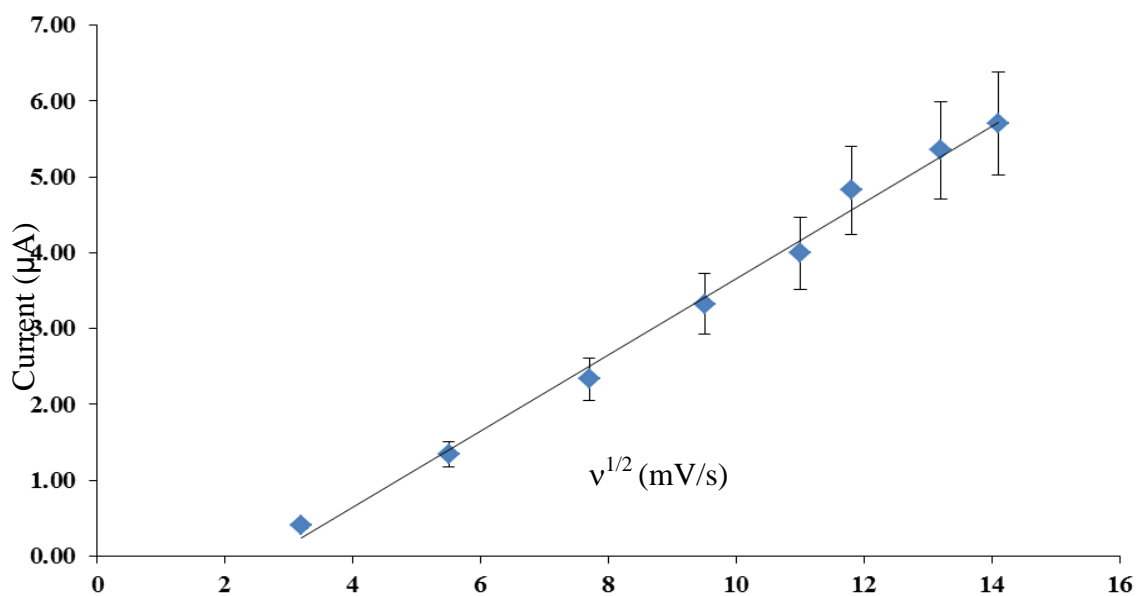


**Figure 7B**

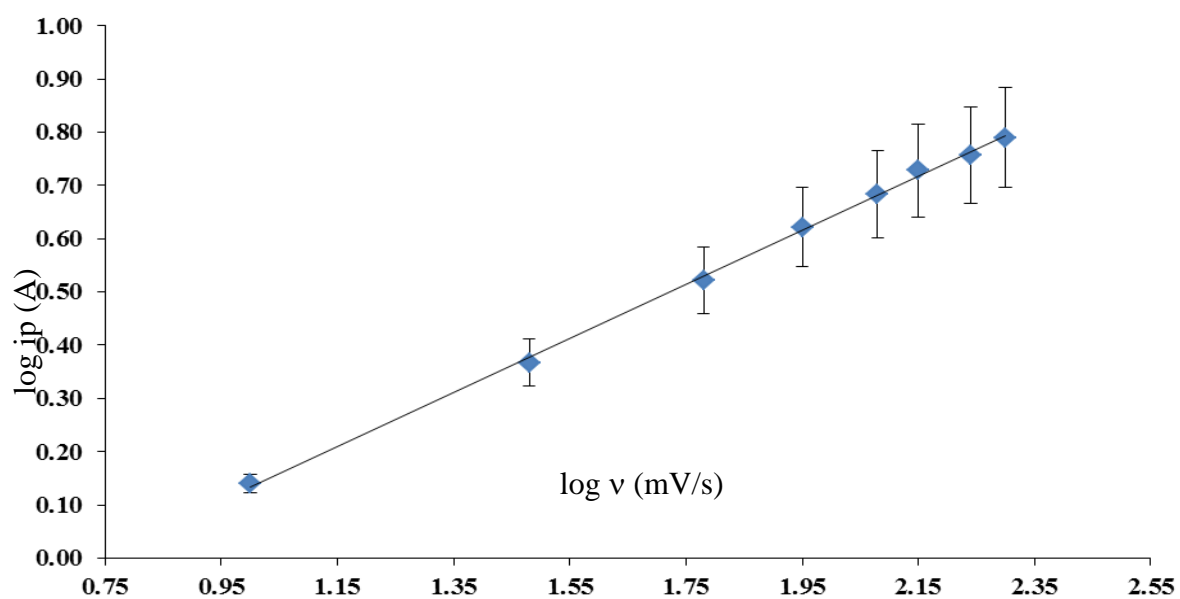


**Figure 7C**

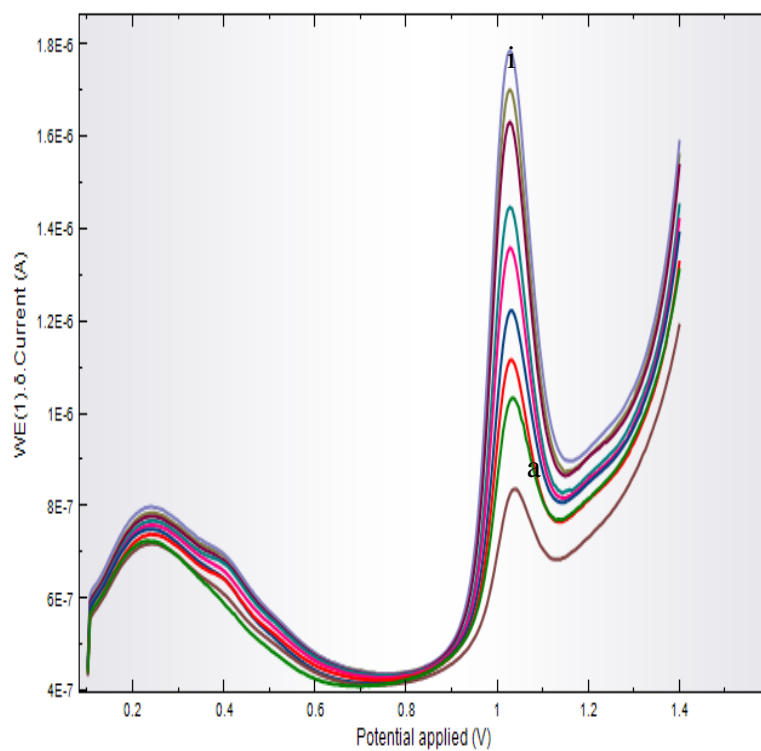


**Figure 8A**

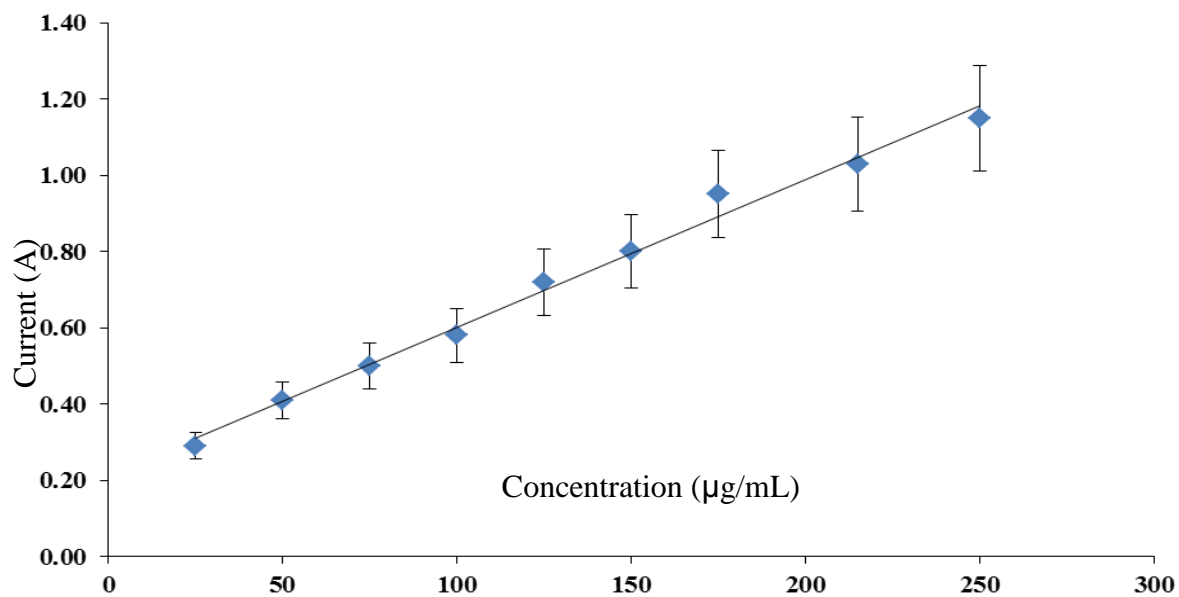


**Figure 8B**